Broad-Spectrum Antimicrobial Polymer with Dual Bactericidal Mechanisms Enhances Antibiotic Activity in the Treatment of Fish Infections

Yue Yu [a], #, Xianhui Chen [a], #, Huangsheng Pu [b, c, d], #, *, Min Wang [a], Junfeng Song [a], Anming Yang [a], Muyang Wan [b], Yugang Bai [a], Qinyun Cai [e], *, Junfa Yuan [f], *Chunhui Zhang [b], * Wing-Leung Wong [g], *, Xinxin Feng [a, h], *

[a] State Key Laboratory of Chemo-/Bio-Sensing and Chemometrics, Hunan Provincial Key Laboratory of Biomacromolecular Chemical Biology, and School of Chemistry and Chemical Engineering, Hunan University, Changsha, Hunan, 410082, China.

[b] College of Biology, Hunan University, Changsha, Hunan, 410082, China.

[c] College of Advanced Interdisciplinary Studies & Hunan Provincial Key Laboratory of Novel Nano Optoelectronic Information Materials and Devices, National University of Defense Technology, Changsha, Hunan 410073, China.

[d] Nanhu Laser Laboratory, National University of Defense Technology, Changsha 410073，China.

[e] State Key Laboratory of Chem/Bio-sensing and Chemometrics, Hunan University, Changsha 410082, P. R. China.

[f] Department of Aquatic Animal Medicine, College of Fisheries, Huazhong Agricultural University, Wuhan 430070, China.

[g] State Key Laboratory of Chemical Biology and Drug Discovery, Department of Applied Biology and Chemical Technology, The Hong Kong Polytechnic University, Hung Hom, Kowloon, Hong Kong SAR 999077, China.

[h] The Third Hospital of Changsha, Hunan Provincial Key Laboratory of Anti-Resistance Microbial Drugs. Changsha, Hunan, 410015, China.

# These authors contributed equally in this work

Correspondence: xinxin_feng@hnu.edu.cn (X.F.), baiyugang@hnu.edu.cn (Y.B.), wing.leung.wong@polyu.edu.hk (W. W.), jfyuan@mail.hzau.edu.cn (J.Y.), phs@nudt.edu.cn (H.P.)

Abstract:

Bacterial infection in aquaculture farming has been a well-known issue, and the situation is worsened by the limitations on antibiotic usage due to environmental considerations. This study reports the design and synthesis of a broad-spectrum antimicrobial polymer, $\mathbf{P_{C3-8}}$, demonstrated for the first time as an efficient antimicrobial agent against a number of common fish pathogens, including Gram-positive and Gram-negative ones. A dual-bactericidal mechanism is proposed for $\mathbf{P_{C3-8}}$, in which the cationic polymer is found to disrupt bacterial membranes and interact with genome DNA, effectively causing bacterial cell death. $\mathbf{P_{C3-8}}$ is capable of eliminating pathogens in mammalian cell cultures, preventing them from being killed by those pathogens. When $\mathbf{P_{C3-8}}$ was applied into water, it healed bacteria-infected zebrafish, outperforming common antibiotics, such as Kanamycin and Chloramphenicol. Importantly, $\mathbf{P_{C3-8}}$ possesses low drug resistance emergence and potent synergistic effects with commercial antibiotics. Therefore, it shows great effectiveness against resistant pathogens and evades any potential environmental risk related to resistance generation. The present study demonstrates that $\mathbf{P_{C3-8}}$ is a promising antimicrobial agent for treating bacterial infection related fish diseases and has potential applications in the aquaculture industry.

1. Introduction

Aquaculture is a huge and essential global food source. (1) However, the emergence of infectious diseases to the aquatic products, particularly in fish farming, (2) not only results in substantial economic losses, but also poses potential health threats to the community. (3) Common fish pathogens include *Acinetobacter baumannii* (*A. b*), *Edwardsiella tarda* (*E. t*), *Escherichia coli* (*E. c*) and *Aeromonas veronii* (*A. v*), (4−7) which frequently cause high morbidity and mortality in fish populations. Moreover, such pathogens also bring threats to humans, (8) as exemplified by *E. t* that not only causes systemic hemorrhagic septicemia with skin lesions in fish, but also is an established human pathogen linked to gastrointestinal, wound, septicemic, and meningeal infections. (9) As a countermeasure, antibiotic usage plays a critical role in aquaculture, but its extensive use poses high risks in promoting antimicrobial resistance (AMR) development in pathogens and indigenous microbiota in aquatic environments. (10,11) Conventional antibiotics are losing efficacy due to AMR, forcing the aquaculture industry to apply antibiotics at higher dosages and creating a deteriorating cycle toward higher AMR risks, (2) because conventional antibiotics being used as the prophylactic and therapeutic agent exert selective pressure and that may play a pivotal role in the selection, persistence, and dissemination of antibiotic-resistant bacteria. (12)

Due to the above AMR issues, some nonantibiotic strategies, including vaccines, probiotics, phytochemicals, and bacteriophages, have been utilized to manage bacterial diseases. (13) Although a number of bacterial vaccines are commercially available for some freshwater species, their efficacy depends entirely on a specific strain that causes disease (14) and is highly sensitive to strain mutations. For probiotics, phytochemicals, and bacteriophages, it is

noteworthy that the inappropriate utilization of microbial agents or disinfectants may pose high risks in disrupting the normal microecology of aquaculture systems, threatening both the environment and the farmed animals. (15) In addition, the limited host range and prevalence of phage-resistant bacteria further hinder the widespread use of phages in aquaculture. (16) Given these limitations, the development of innovative, broad-spectrum, and antiresistance antibacterial agents is imperative. Such antimicrobial agents with unprecedented antiresistance mechanisms also feature great market values; however, to develop these desirable antimicrobial agents is apparently a challenging task due to the requirements of introducing innovative antimicrobial approaches.

A potential solution has been gradually revealed in recent years because some polymer-based new antimicrobials are developed and used as promising alternatives to conventional prophylactic and therapeutic agents. (17) In addition, employing a multitargeting approach, some antimicrobials may achieve better antibacterial efficacy than those single-targeting therapeutic agents and provide advantages in antiresistance properties. (18−22) For example, dual-targeting oligoguanidines and oligoamidines were reported (23) to be capable of disrupting bacterial membrane integrity and DNA activity via strong molecular interactions, showing high and broad-spectrum antimicrobial effectiveness against normal and resistant bacterial strains and causing no resistance generation after being used frequently. Based on these understandings, we propose that a suitable optimization of the amphiphilic polymers may provide effective antibacterial agents to address the current challenges of infection treatments and multidrug resistance in aquaculture farming. In the present study, we reported the development of polymeric peptidomimetics, which were further optimized from our previous molecular designs, (23) and demonstrated that a cationic polymeric compound, $\mathbf{P_{C3–8}}$, was a potent hit for treating bacterial infections in fish. In addition to its antimicrobial properties, $\mathbf{P_{C3–8}}$ was found to be able to provide notably synergistic effects with conventional antibiotics to enhance antibacterial efficacy. A detailed investigation of $\mathbf{P_{C3–8}}$ in the mechanism of action, in vitro antibacterial property, and in vivo therapeutic efficacy against the major fish pathogens was also conducted (Figure 1). With excellent selectivity in targeting the bacterial membrane and DNA, the cationic polymeric compound, $\mathbf{P_{C3–8}}$, shows promising antibacterial performance and resistance-resistant ability as the effective disinfection and therapeutic agent against fish bacterial pathogens.

2. Experimental Section

2.1. Materials

2.1.1. Chemical Reagents

Unless otherwise stated, all chemicals were obtained from Sigma-Aldrich (USA), Macklin Chemical (Shanghai, China), and Leyan (Shanghai, China).

2.1.2. Biological Reagents

Plasmid DNA pCold-ctxm-15 was a kind gift from Prof. Jing Huang. Water was generated using a Milli-Q water purifier.

2.2. Bacterial Strains and Cell Lines

The following bacteria were sourced from the American Type Culture Collection (ATCC, Manassas, VA): *E. c* (K12, ATCC 29425); *Bacillus subtilis* from subsp. subtilis (Ehrenberg) Cohn (ATCC 6051); *Mycobacterium smegmatis* MC2 155 (ATCC 700084); *Enterococcus faecalis* (Andrewes and Horder) Schleifer and Kilpper-Balz (ATCC 19433); *Staphylococcus aureus* Newman strain (ATCC 25904); *Klebsiella pneumoniae* subsp. pneumoniae Schroeter Trevisan (ATCC 27736); *A. b* (Bouvet and Grimont, ATCC 19606); *Pseudomonas aeruginosa* PA01 (ATCC 47085); and *E. tarda* (GIM1.397). *Micropterus salmoides-Aeromonas hydrophila* (MS-*A. h*), *M. salmoides-Plesiomonas Shigelloides* (MS-*P. s*), *M. salmoides-A. veronii* (MS-*V. h*), and *M. salmoides-E. dwardsiella* (MS-*E. d*) were obtained from Huazhong Agricultural University. Clinical isolates of bacteria were acquired from the hospitals of Peking University and Shenzhen People's Hospital. Murine embryonic fibroblast cell line NIH/3T3 (ATCC CRL-1658) were purchased from ATCC.

2.3. Instrumentation

Analytical gel permeation chromatography (GPC): GPC analyses were conducted on a Waters system featuring a Waters 515 isocratic pump and a Waters 2414 refractive index detector. Separations were performed at 40 °C using an aqueous solution of $NaNO_3$ (0.01 M) as the mobile phase.

Flow cytometry study: flow cytometry studies were carried out using a Becton Dickinson Accuri C6 Plus instrument. Green fluorescence was detected with an excitation of 488 nm and an emission of 533 ± 30 nm, while red fluorescence was detected with an excitation of 488 nm and an emission of 585 ± 30 nm. Fluorescence signals were quantified by the geometric mean. Data underwent processing in FlowJo and were subsequently aligned and annotated using Adobe Illustrator CC.

Confocal microscopy: fluorescence microscopy images were captured using a Nikon Eclipse Ti2-E Laser Confocal Microscope. Excitation wavelengths were set at 405 nm for blue fluorescence, 488 nm for green fluorescence, and 561 nm for red fluorescence.

2.4. Minimum Inhibitory Concentration Measurement

An antimicrobial susceptibility evaluation was conducted based on a standard microdilution protocol. (24) Bacterial cultures were prepared by diluting an overnight culture of the test pathogen in CAMHB, followed by regrowth to mid logarithmic phase. The resulting suspension was diluted to 5×10^5 CFU/mL and allocated to wells containing 2-fold serial dilutions of $\mathbf{P_{C3-8}}$ (0.25–32 μg/mL) or conventional antibiotics. Microtiter plates were incubated under shaking conditions for 16–24 h at

37 °C. Bacterial growth inhibition was quantified by measuring optical density at 600 nm to define minimum inhibitory concentration (MIC) values based on triplicate experiments.

2.5. MTT Assay

The cytotoxic effect of the oligoamidine was examined in murine embryonic fibroblast cell line NIH/3T3 using an MTT colorimetric assay. Cells were seeded at 1×10^4 cells per well and exposed to varying concentrations of the test compounds in the culture medium for 24 h. Untreated controls were included for comparison. After incubation, the medium was removed, cells were rinsed with PBS, and fresh medium containing 0.5 mg/mL MTT was added for 1.5 h of staining. Formazan production was solubilized with DMSO and the absorbance measured at 600 nm. Cell viability was calculated by normalizing the absorbance of treated samples to untreated controls.

2.6. Lipid and DNA Interference on MIC

Bacterial cultures were prepared as described in the MIC protocol and supplemented with 128 μg/mL of lipopolysaccharide (LPS), phosphatidylglycerol (PG), or salmon sperm DNA prior to allocation into microtiter plates. Serial dilutions of test agents were added and the samples were incubated under standard MIC conditions. Growth inhibition was evaluated by optical density quantification as described above.

2.7. Bacterial Membrane Permeability Assay

E. c cultures were harvested, washed with PBS, and resuspended ($OD_{600\,nm}$ = 0.1) in media containing propidium iodide (PI) (100 μM). Bacteria were exposed to specified concentrations of $\mathbf{P_{C3–8}}$ or the controls and incubated (37 °C, 2 h). Membrane damage was assessed by flow cytometry analysis of cells exhibiting red fluorescence upon dye entry; 10^4 events per sample were analyzed.

2.8. Gel Retardance Assay

Compounds were mixed with pCold-ctx-m-15 plasmid DNA or genomic DNA in PBS (pH 7.4) and incubated at 25 °C for 30 min. The genomic DNA was extracted from *E. coli* cells using the Universal Genomic DNA Purification Mini Spin Kit (Beyotime) according to the manufacturer's instructions. Resulting complexes were separated by agarose gel electrophoresis (1%, 40 min) with Gelred (2 μg/mL), visualized under ultraviolet light, and imaged. Alterations in DNA migration indicating binding interactions were quantified by grayscale density evaluation with ImageJ software.

2.9. Fluorescence Titration Experiment

Preformed complexes of pCold-ctx-m-15 (10 μg/mL) and PI (1 μg/mL) were prepared in PBS (37 °C for 30 min). Incremental concentrations of $\mathbf{P_{C3–8}}$ were added and equilibrated (37 °C, 1 h) prior to measuring fluorescence emission spectra on mixtures before and after addition. Changes in the PI fluorescence suggest compound-mediated displacement from DNA binding.

2.10. Confocal Microscopy of $\mathbf{P_{C3–8}}$-Stained Cells and Bacteria

Fluorescently labeled $\mathbf{P_{C3–8}}$-RhB was incubated with NIH/3T3 cells and *A. b*-MDR bacteria to visualize the cellular and bacterial distribution. $\mathbf{P_{C3–8}}$-RhB (8 μg/mL) was incubated with NIH/3T3 cells in Dulbecco's modified Eagle media supplemented with 10% fetal bovine serum for 24 h and with *A.*

b-MDR bacteria in PBS for 2 h. After washing, Hoechst staining, DiO staining of bacteria, and paraformaldehyde fixing occurred. Localization of $\mathbf{P_{C3-8}}$-RhB in cells and bacteria was determined through colocalization of fluorescent labels (green DiO, blue Hoechst, and red $\mathbf{P_{C3-8}}$-RhB) using confocal microscopy.

2.11. RT-PCR Study of recA

For this experiment, 0.5 × MIC $\mathbf{P_{C3-8}}$ was added to different groups of *S. aureus* (*S. a*) and *A. b*. The total RNA of *S. a* or *A. b* was extracted using the HiPure Bacterial RNA Kit (Magen, Shanghai), following the manufacturer's instructions. The total amount of RNA extracted for each group was quantified by using Nanodrop. The RT-PCR assay was conducted in a real-time PCR system (QuantStudio 7 Flex, Thermo Fisher Scientific, USA) with the HiScript II One Step qRT-PCR SYBR Green Kit (Vazyme, Nanjing). Gene expression was normalized to the expression of the housekeeping gene (16S rRNA). The primer sequences for each gene are listed in Table S1.

2.12. Reactive Oxygen Species Generation Assay

Bacterial cultures were cultured, washed, and resuspended in PBS. The bacterial suspension was diluted to $OD_{600\,nm}$ = 0.2, mixed with 5 μM DCFH-DA dye, and treated with $\mathbf{P_{C3-8}}$ for 3 h at 37 °C in the dark. Reactive oxygen species (ROS) generation was analyzed immediately using flow cytometry to detect fluorescence of the ROS-sensitive dye (Ex 488 nm, Em 533 nm).

2.13. Time-Kill Assay

Bacterial cultures (*A. b*) were prepared as described for the MIC testing. At early logarithmic phase, aliquots were treated with serial dilutions of test compounds. Immediately after addition (0 h) and at designated time points, samples were collected, serially diluted, and plated to quantify viable colonies (CFU/mL) following overnight incubation.

2.14. Resistance Generation Assay

A multistep resistance selection protocol was conducted based on previously reported methods. (23) *E. c* was propagated for 18 days in subinhibitory compound concentrations, with daily refreshing of media and standardization of inoculum density. MICs were tracked for each passage by microdilution susceptibility testing. A ≥4-fold increase over the baseline MIC was considered indicative of acquired resistance.

2.15. Checkerboard Assay

Bacterial cultures were prepared as described above and allocated to microtiter plates. Dilutions of each single agent or pair of compounds were added to the wells in orthogonal orientations. Following incubation, the optical density was measured to determine MIC values. Fractional inhibitory concentration indices (FICi) were calculated for each combination using the equation:

$$\mathrm{FICi} = \frac{\mathrm{MIC_{ac}}}{\mathrm{MIC_a}} + \frac{\mathrm{MIC_{bc}}}{\mathrm{MIC_b}} = \mathrm{FIC_a} + \mathrm{FIC_b}$$

where MIC_a and MIC_{ac} are the MICs of compound alone and combined with compound c, respectively; MIC_b and MIC_{bc} represent the MIC of compound b alone, and combined with

compound c, respectively. FICi ≤ 0.5 indicates synergism between the two agents. Assays were conducted with a minimum of two biological duplicates.

2.16. Synergistic Mechanism Study

Following the same sample preparation method as described previously in Sections 2.7 and 2.11, the bacterial suspension was mixed with the combination of $\mathbf{P_{C3-8}}$ (1 μg/mL for the membrane permeability assay and 1 μg/mL for the ROS generation assay) and different concentrations of Niclosamide.

2.17. Evaluation of Cytotoxicity Using a Coculture Model

Mammalian cytotoxicity was evaluated using a coculture model of NIH/3T3 fibroblasts and *A. b*-MDR. Cells were propagated to confluence in 24-well plates before infection with 10^6 CFU bacteria and simultaneous addition of test agents ($\mathbf{P_{C3-8}}$, 8 μg/mL; Gentamicin, 8 μg/mL) or PBS control. Following 24 h incubation, cocultures were examined microscopically and aliquots collected to quantify viability by trypan blue exclusion. Bacterial burden was determined by serial dilution plating. Cell viability was calculated as viability % = (treatment cell count/uninfected control cell count) × 100%. To demonstrate the synergistic effect in the coculture model, a combination of $\mathbf{P_{C3-8}}$ (1 μg/mL) and Niclosamide (8 μg/mL) was added.

2.18. Zebrafish Infection Model

First, 50 adult blue zebrafish (weight about 0.3 g) were scratched using a surgical knife and then randomly divided into 4 groups: PBS group, chloramphenicol group, Kanamycin group, and $\mathbf{P_{C3-8}}$ group, and transferred into 500 mL beakers containing 150 mL sterile water, respectively. The $OD_{600\ nm}$ value of the overnight cultured *E. t* bacteria solution was measured, and the number of CFU was calculated based on the relationship between $OD_{600\ nm}$ and CFU of *E. t*. 5×10^7 CFU/mL bacteria solution was added into each beaker. Subsequently, 2 μg/mL of the corresponding antibacterial agents were added into each beaker, then the survival of zebrafish in each group was monitored. After infection and treatment for 8 h, the bacteria-containing water was replaced with sterile water, then water was changed every 24 h, and the continuous recording of zebrafish survival. The experiment was terminated after 10 days and the survival curves were plotted.

3. Results and Discussion

3.1. Screening of Active Polymers against *E. t*. Infection

E. t is one of the primary contributors to the disease known as edwardsiellosis and poses major challenges for clinical treatment and aquaculture. (7) *E. t* invades and multiplies within epithelial cells and macrophages and evades host immunity to persist in fish. (25) Because of its intracellular parasitism and environmental adaptability, *E. t* was selected as a model for the screening study. Two categories of polymers (Figure 2), $\mathbf{P_{C3}}$ series and $\mathbf{P_{C4}}$ series, were synthesized (26) and screened against *E. t*. The screening results summarized in Table 1 show MIC against *E. t*. Both $\mathbf{P_{C3-8}}$ and $\mathbf{P_{C3-6}}$ gave potent antibacterial activities with MIC down to 4 μg/mL. Moreover, toxicity evaluation of the polymers in mammalian NIH3T3 cells revealed that $\mathbf{P_{C3-8}}$ had higher IC_{50} values compared to $\mathbf{P_{C3-}}$

$_6$ (Table S2). Given its potent activity against *E. t* and lower toxicity, $\mathbf{P_{C3–8}}$ was prioritized for further investigations.

Additionally, $\mathbf{P_{C3–8}}$, with a determined molecular mass of 3040 Da by using GPC analysis (Figure S1), displayed a remarkable antibacterial activity against perch fish pathogens, including MS-*A. h*, MS-*P. h*, MS-*V. h*, and MS-*E. d*, which were obtained from Huazhong Agricultural University. The MIC values were found to be 1–3 μg/mL. From these results, $\mathbf{P_{C3–8}}$ exhibited robust and wide-ranging antibacterial efficacy against various pathogenic bacteria.

3.2. $\mathbf{P_{C3–8}}$ Shows Dual Antibacterial Mechanisms

Similar to our previously reported oligomers, (23,27−29) $\mathbf{P_{C3–8}}$ also exhibited a dual mechanism of action in killing pathogenic bacteria. We first investigated their binding affinity toward bacterial membranes. The antibacterial activity of $\mathbf{P_{C3–8}}$ was evaluated in the presence of essential exogenous membrane components, including PG and LPS, was assessed. (30,31) As shown in Figure 3A, upon the addition of 128 μg/mL LPS or PG, the bactericidal activity of $\mathbf{P_{C3–8}}$ was significantly reduced, indicating that $\mathbf{P_{C3–8}}$ interacted with LPS and PG. Additionally, the lytic effect of $\mathbf{P_{C3–8}}$ on the bacterial membrane may enhance its permeability to bacterial cells. The effect can be demonstrated with the increased delivery of a membrane-impermeable dye, PI, into the bacterial cells. When PI was delivered into the bacterial cells, it intercalated with DNA and produced red fluorescence that could be quantified with flow cytometry. From the assay, by comparing the PI fluorescence of *E. c* treated with $\mathbf{P_{C3–8}}$ and the control group (untreated), it was found that a notable fluorescence was increased, as depicted in Figure 3B. This enhanced permeabilization action is presumably able to facilitate the accumulation of $\mathbf{P_{C3–8}}$ in bacterial cells, and thus more polymeric molecules could bind to DNA.

To validate the interaction of $\mathbf{P_{C3–8}}$ with DNA, we conducted Gel retardation assays were conducted. $\mathbf{P_{C3–8}}$ at the concentration higher than 32 μg/mL exhibited robust binding to both the plasmid DNA (pCold-ctx-m-15) and genomic DNA, resulting in complete inhibition of migration for 96% of the plasmid DNA and 94% of the genomic DNA on the gel (Figuress 3C and S2). The antibacterial activity of $\mathbf{P_{C3–8}}$ against *E. c* could also be inhibited by adding genomic DNA, while the addition of DNA in the control experiment using a membrane-targeting antibiotic colistin shows no effects (Figure S3). The results suggest that $\mathbf{P_{C3–8}}$ may interact with the exogenous DNA added. Thus, a reduction in the antibacterial ability was observed. On the contrary, Colistin is a non-DNA targeting antibiotic and it is therefore not affected by the exogenous DNA added. These results were also consistent with the fluorescence titration experiments, in which adding $\mathbf{P_{C3–8}}$ disrupted the PI–DNA complex, displacing the bound PI and markedly decreasing fluorescence. It was found that about 75% of PI was displaced by $\mathbf{P_{C3–8}}$ (at 16 μg/mL). Almost 100% PI displacement could be achieved under high $\mathbf{P_{C3–8}}$ concentration conditions (50–100 μg/mL) (Figure 3D).

To further test the hypothesis that $\mathbf{P_{C3–8}}$ could bind to DNA within bacterial nucleoids, we incubated bacterial cells (*A. b*) with $\mathbf{P_{C3–8}}$-RhB and visualized the cellular location of the molecule by confocal microscopy. $\mathbf{P_{C3–8}}$-RhB was also costained and with Hoechst dye, a nucleoid-specific stain. The results showed a well colocalization of both dyes in the nucleus and provided cellular evidence to

support the DNA-targeted mechanism of $\mathbf{P_{C3–8}}$ in antibacterial action (Figures 3E and S4). In contrast, in the murine embryonic fibroblast cell line NIH/3T3, $\mathbf{P_{C3–8}}$-RhB did not penetrate the nuclear membrane, probably due to its large molecular size. The nuclear membrane impermeability of $\mathbf{P_{C3–8}}$ in NIH/3T3 cells might reduce its cytotoxicity to human cells. The bacterial membrane-selective property of $\mathbf{P_{C3–8}}$ might increase its practical potential for being used as an antibiotic against bacterial infections.

It is well established that considerable DNA damage within the bacterial chromosome can trigger the activation of the SOS response. Within this response, perturbations in the DNA structure enhance the expression and activity of the recA protease. (32) This, in turn, initiates an error-prone translesion DNA synthesis mechanism aimed at repairing DNA damage. Hence, activation of the recA gene becomes indicative of the extent of DNA damage following chemical exposure. Notably, our investigation has unveiled a significant upregulation in recA gene expression in the treatment group compared to the untreated control group (Figure S5).

To quantify ROS production in *E. c* treated with different concentrations of $\mathbf{P_{C3–8}}$, we employed a dichlorofluorescein diacetate (DCFH-DA), a ROS-sensitive probe, and conducted flow cytometry analysis. As shown in Figures 4A and S6, $\mathbf{P_{C3–8}}$ induced ROS in both Gram-negative and Gram-positive bacterial cells, including *E. c* (Figure 4A) and *B. s* and *S. a* (Figure S6A,B).

While DCFH-DA detects overall ROS levels, we additionally used dihydroethidium (DHE), a superoxide anion (O_2^-) specific probe, to investigate this particular ROS in *E. c*. The data revealed that $\mathbf{P_{C3–8}}$ exposure also led to an increase of O_2^- levels (Figure S6C). Enhancing cellular ROS production is a well-established antibiotic-mediated sterilization mechanism. (33,34) ROS production likely represents one of the mechanisms underlying the membrane disrupting and DNA binding effects of $\mathbf{P_{C3–8}}$. (35) As shown in Figure 4B, $\mathbf{P_{C3–8}}$ also showed rapid bactericidal kinetics. *A. b* and *A. b*-MDR (Figure S7) treated with $\mathbf{P_{C3–8}}$ at 1 × MIC were completely killed within half an hour. Compared with most conventional antibiotics, $\mathbf{P_{C3–8}}$ generally exhibited superior bactericidal activity against antibiotic-resistant strains. In addition, from the resistance evolution profiles for $\mathbf{P_{C3–8}}$ (Figure 4C), it shows no notable drug-resistance developed compared to the traditional antibiotics like Gentamicin and Ampicillin, which give more than 15-fold MIC increments over an 18 day experiment. Moreover, under antibiotic selection pressure, $\mathbf{P_{C3–8}}$ retained antibacterial efficacy throughout the entire evolutionary process. Additionally, when extending our analysis to include other bacterial strains, such as *E. t*, *B. s*, and *S. a* (Figure S8), the resistance evolution profiles for $\mathbf{P_{C3–8}}$ remained consistent. Notably, $\mathbf{P_{C3–8}}$ maintained its antibacterial efficacy against a broad spectrum of bacterial strains throughout the entire evolutionary process.

3.3. $\mathbf{P_{C3–8}}$ Enhances Antibiotic Sensitivity against Drug-Resistant *A. b*

Certain cationic, amphiphilic polymers with membrane-disrupting properties can enhance the efficacy of antibiotics against pathogenic bacteria. (36,37) A combination therapy may be advantageous in aquaculture settings, as polymeric sensitizers have the potential to enhance the efficacy of currently utilized antibiotics, thereby reducing the required antibiotic dosage for effective

treatment. *A. b* is a Gram-negative opportunistic bacterium that has spread globally. (38) Emerging evidence suggests that this pathogen is a deadly threat to fish and its presence increases the risk of infections in fish populations. (5)

To investigate whether $\mathbf{P_{C3-8}}$ could potentially act as a sensitizer, we systematically screened the effectiveness of 33 regular antibiotics against *A. b*, with or without the addition of $\mathbf{P_{C3-8}}$ at a subinhibitory concentration (1/4 MIC). The antibiotic combined with $\mathbf{P_{C3-8}}$ showing a 2-fold or higher MIC reduction was considered as a hit for synergy (Figure 5A, Table S4). Following this, checkerboard assays were conducted on the initial hits, utilizing the fractional inhibitory concentration index (FICi) to quantitatively assess the synergistic effect between the antibiotic and $\mathbf{P_{C3-8}}$. Using the FICi calculate method, FICi values of ≤0.5 represent synergism and >0.5 represents drug antagonism.

The FICi values were determined to be 0.31 for Niclosamide (Figure 5B), 0.31 for aminoglycoside Gentamicin (Figure S9A), 0.28 for the Erythromycin (Figure S9B), and 0.31 for Valnemulin (Figure S9C). Moreover, the screening study included the clinical strains of *A. b* and the drug-resistant isolate *A. b*-MDR (Figure S10A). We found that $\mathbf{P_{C3-8}}$ exhibited promising synergistic effects when combined with clinically relevant antibiotics, such as Rifampin and Valnemulin, with FICi values as low as 0.25 and 0.5, respectively (Figure S10B,C).

Because Niclosamide is a clinically approved drug and has been utilized for treating helminth parasites in both humans and animals, (39) we further explored the synergistic mechanism between $\mathbf{P_{C3-8}}$ and Niclosamide. The results strongly support a synergistic mechanism of action for $\mathbf{P_{C3-8}}$ and the Niclosamide combination treatment, which involves membrane targeting (Figure 5C) and the induction of ROS (Figure 5D). To quantify ROS production in *E. t* treated with a combination of $\mathbf{P_{C3-8}}$ and Niclosamide at different concentrations, we employed a dichlorofluorescein diacetate (DCFH-DA) probe (a ROS indicator) and conducted flow cytometry analysis. Our results revealed a significant increase in the ROS level in bacteria for the combination treatment compared to the untreated bacteria. Furthermore, compared to the single drug treatment, Niclosamide upon combining with $\mathbf{P_{C3-8}}$ (1 μg/mL) significantly reduced its MIC (4-folds), suggesting a potent synergistic effect. Thus, $\mathbf{P_{C3-8}}$ could increase the sensitivity of antibiotics, while the antibiotic also enhances the bactericidal effect of $\mathbf{P_{C3-8}}$. These results further support the potential of $\mathbf{P_{C3-8}}$ as a multitarget antibacterial agent for treating infections. The reduction in MIC values observed in these clinical strains aligns with our observations in Table 2, emphasizing the capability of $\mathbf{P_{C3-8}}$ as a potent bactericidal agent and sensitizer.

3.4. Ex Vivo and in Vivo Assessments to Demonstrate the Therapeutic Potential of P_{C3-8} against Bacteria-Associated Infections

To evaluate the antimicrobial therapeutic potential of $\mathbf{P_{C3-8}}$, we conducted antibacterial experiments in vitro and also established an ex vivo coculture model of bacteria and NIH/3T3 cells as well as the in vivo model of zebrafish infection. In the ex vivo coculture model, mouse fibroblasts NIH/3T3 cells were infected with a clinical multidrug-resistant *A. b* isolate (Figure 6A). Without any treatment, *A. b* proliferated rapidly within 24 h and killed most cells (viability <20%, Figure 6B). The

treatment with the antibiotic Gentamicin alone failed to eliminate the bacteria infecting the cells. However, with the addition of $\mathbf{P_{C3-8}}$ at 8 μg/mL, the bacteria were completely cleared (Figure 6C) and the cells were restored to a normal morphology. The cell viability was increased to approximately 60%. Apparently, $\mathbf{P_{C3-8}}$ exhibited high activity and selectivity in this setting by killing pathogens and rescuing the cells. Importantly, the coculture model demonstrated the stability and activity of the active component of $\mathbf{P_{C3-8}}$ in serum, a crucial aspect for its effective application in vivo. In Figure 5, we demonstrate the significant synergistic effect of $\mathbf{P_{C3-8}}$ and Niclosamide. We thus applied a coculture model to verify this synergistic effect in an infection setting. In the model, mouse fibroblasts NIH/3T3 cells were infected with *E. t* isolate (Figures 7A, S11). *E. t* without any treatment proliferated rapidly within 12 h and most NIH/3T3 cells were killed (viability <10%, Figure 7B). For the treatment with Niclosamide alone, it failed to eliminate the bacteria infecting the cells (Figure 7C). However, when combining Niclosamide and $\mathbf{P_{C3-8}}$ (at 1 μg/mL) for the treatment, the bacteria in NIH/3T3 cells were completely killed and the cells were restored to a normal morphology (Figure 7A). Cell viability was found to increase to approximately 70% (Figure 7B). Again, $\mathbf{P_{C3-8}}$ exhibited high activity and selectivity in eradicating pathogens and successfully rescued the *E. t*-infected cells. The result of this coculture model further supports the strong antimicrobial activity and biocompatibility of $\mathbf{P_{C3-8}}$ in NIH/3T3 cells.

Furthermore, a zebrafish model was employed to evaluate the in vivo toxicity and therapeutic potential of $\mathbf{P_{C3-8}}$ against bacterial infections. We developed a zebrafish wound model to assess the effectiveness of $\mathbf{P_{C3-8}}$. In the experiments, an artificial scratch wound (4 × 5 mm) was created on each fish by removing scales and skin and followed by transferring to water. We selected *E. t* as a model pathogen and simulated natural pond contaminations by direct addition to the water (Figure 8A). $\mathbf{P_{C3-8}}$ and other antibiotics were then introduced into the water for treatment. In the untreated group, 75% mortality occurred by 24 h (Figure 8B). For the treatment with chloramphenicol, it resulted in approximately 60% mortality by 24 h, indicating an ineffective treatment against *E. t*. Even Kanamycin, an *E. t*-sensitive antibiotic, showed only 50% mortality by 100 h. In contrast, $\mathbf{P_{C3-8}}$ (2 μg/mL) successfully rescued 100% of the *E. t*-infected zebrafish. These results strongly demonstrate that $\mathbf{P_{C3-8}}$ is a highly promising candidate, capable of clearing pathogens and safely rescuing infected animal models, showing broad-spectrum activity, high drug resistance and excellent therapeutic effects, and low toxicity in simulated natural environments.

4. Conclusions

In conclusion, we developed a broad-spectrum antimicrobial polymer $\mathbf{P_{C3-8}}$ and demonstrated its potent inhibitory effects against a number of Gram-positive and Gram-negative bacteria, especially the common fish pathogens including *E. t*. $\mathbf{P_{C3-8}}$ demonstrates powerful antibacterial effects through dual-selective mechanisms, specifically by selectively disrupting bacterial cell membranes and binding selectively to bacterial DNA. Both in vitro and in vivo experiments showed that $\mathbf{P_{C3-8}}$ could effectively clear pathogens and rescue bacteria-infected NIH/3T3 cells and zebrafish.

Furthermore, $\mathbf{P_{C3-8}}$ exhibited low resistance development and strong synergistic effects with conventional antibiotics like Niclosamide. Based on these results, $\mathbf{P_{C3-8}}$ shows great potential to be a highly promising therapeutic agent for preventing and treating bacterial diseases in fish. Additionally, it demonstrates the potential for combination therapy with existing antibiotics, enabling reduced toxicity and drug repurposing. The molecular design of $\mathbf{P_{C3-8}}$ may provide insights into the development of antimicrobial agents for aquaculture applications. Further studies will be conducted to understand more about the physical, chemical, and biological properties of $\mathbf{P_{C3-8}}$ and its related antimicrobial polymers including solubility, stability, and the effect of varying molecular mass of the polymer. These investigations aim to enhance the efficacy and safety profile of $\mathbf{P_{C3-8}}$. Ultimately, its potential for being used as a practical therapeutic against bacterial infections in aquatic environments can be strengthened.

Author Contributions

Y.Y., X.C. and H.P, contributed equally in this work. Y.Y., X.C., H.P., M.W., J.S., and A.Y. conducted research. All authors contributed in data analysis. Y.Y., X.C., Q.C., W.L.W., Y.B., and X.F. wrote the paper. H.P., J.Y., M.W., C.Z., W.L.W., Y.B., and X.F. contributed to the funding.

Funding

We acknowledge the financial supports received from the funding agents including the National Key Research and Development Program of China (2023YFD1800100 to X.F. and Y.B.), National Natural Science Foundation of China (Grants 22177031 to X.F., 92163127 to Y.B, 82102415 to M.W., and 82304277 to C.Z., 32073013 to J.Y.), the Natural Science Foundation of Hunan Province (2024JJ4007 to X.F., 2022RC1107 and 2024JJ2010 to Y.B.), the project of Hunan Provincial Key Laboratory of Anti-Resistance Microbial Drugs (2023TP1013 to X.F.), the Natural Science Foundation of Changsha (kq2208050 to C.Z.), the Independent Research Project of the College of Advanced Interdisciplinary Studies of NUDT (22-ZZKY-03 to H.P.), and the Health and Medical Research Fund (HMRF, Project No.: 22210412 to W.L.W.), Hong Kong SAR.

Notes

The authors declare no competing financial interest.

Acknowledgments

The authors thank the Analytical Instrumentation Center of Hunan University for flow cytometry support. We are grateful to M.W. for her assistance with the RT-PCR study of *recA* expression.

References

1. Ahmad, A.; Abdullah, S. R. S.; Abu Hasan, H.; Othman, A. R.; Ismail, N. I. Aquaculture industry: Supply and demand, best practices, effluent and its current issues and treatment technology. J. Environ. Manage. 2021, 287, 112271, DOI: 10.1016/j.jenvman.2021.112271
2. Deekshit, V. K.; Maiti, B.; Krishna Kumar, B.; Kotian, A.; Pinto, G.; Bondad-Reantaso, M. G.; Karunasagar, I.; Karunasagar, I. Antimicrobial resistance in fish pathogens and alternative risk mitigation strategies. Rev. Aquacult. 2023, 15 (1), 261– 273, DOI: 10.1111/raq.12715
3. Subasinghe, R. Disease control in aquaculture and the responsible use of veterinary drugs and vaccines: the issues, prospects and challenges. Options Mediterr. 2009, 86, 5–11
4. Guzman, M. C.; Bistoni, M. d. l. A.; Tamagnini, L. M.; Gonzalez, R. D. Recovery of Escherichia coli in fresh water fish, Jenynsia multidentata and Bryconamericus iheringi. Water Res. 2004, 38 (9), 2367– 2373, DOI: 10.1016/j.watres.2004.02.016
5. Xia, L.; Xiong, D.; Gu, Z.; Xu, Z.; Chen, C.; Xie, J.; Xu, P. Recovery of Acinetobacter baumannii from diseased channel catfish (Ictalurus punctatus) in China. Aquaculture 2008, 284, 285–288, DOI: 10.1016/j.aquaculture.2008.07.038
6. Novotny, L.; Dvorska, L.; Lorencova, A.; Beran, V.; Pavlik, I. Fish: a potential source of bacterial pathogens for human beings. Vet. Med. 2004, 49 (9), 343– 358, DOI: 10.17221/5715-VETMED
7. Xu, T.; Zhang, X. Edwardsiella tarda: an intriguing problem in aquaculture. Aquaculture 2014, 431, 129– 135, DOI: 10.1016/j.aquaculture.2013.12.001
8. Sanito, R. C.; Yeh, T.-H.; You, S.-J.; Wang, Y.-F. Novel TiO2/PANI composites as a disinfectant for the elimination of Escherichia coli and Staphylococcus aureus in aquaculture water. Environ. Technol. Innovat. 2021, 22, 101502, DOI: 10.1016/j.eti.2021.101502
9. Janda, J. M.; Abbott, S. L. Infections associated with the genus Edwardsiella: the role of Edwardsiella tarda in human disease. Clin. Infect. Dis. 1993, 17 (4), 742– 748, DOI: 10.1093/clinids/17.4.742
10. Schar, D.; Zhao, C.; Wang, Y.; Larsson, D. G. J.; Gilbert, M.; Van Boeckel, T. P. Twenty-year trends in antimicrobial resistance from aquaculture and fisheries in Asia. Nat. Commun. 2021, 12 (1), 5384, DOI: 10.1038/s41467-021-25655-8
11. Caputo, A.; Bondad-Reantaso, M. G.; Karunasagar, I.; Hao, B.; Gaunt, P.; Verner-Jeffreys, D.; Fridman, S.; Dorado-Garcia, A. Antimicrobial resistance in aquaculture: A global analysis of literature and national action plans. Rev. Aquacult. 2023, 15 (2), 568– 578, DOI: 10.1111/raq.12741
12. Cabello, F. C.; Godfrey, H. P.; Tomova, A.; Ivanova, L.; Dölz, H.; Millanao, A.; Buschmann, A. H. Antimicrobial use in aquaculture re-examined: its relevance to antimicrobial resistance and to animal and human health. Environ. Microbiol. 2013, 15 (7), 1917– 1942, DOI: 10.1111/1462-2920.12134

13. Perez-Sanchez, T.; Mora-Sanchez, B.; Luis Balcazar, J. Biological Approaches for Disease Control in Aquaculture: Advantages, Limitations and Challenges. Trends Microbiol. 2018, 26 (11), 896–903, DOI: 10.1016/j.tim.2018.05.002
14. Ma, J.; Bruce, T. J.; Jones, E. M.; Cain, K. D. A Re of Fish Vaccine Development Strategies: Conventional Methods and Modern Biotechnological Approaches. Microorganisms 2019, 7 (11), 569, DOI: 10.3390/microorganisms7110569
15. Heloísa, T.; Farias, V.; Levy-Pereira, N.; Alves, O.; de, D.; Dias, C.; c, L. T.; Pilarski, F.; Belo, M. A. A.; José, M.Probiotic feeding improves the immunity of pacus, Piaractus mesopotamicus, during Aeromonas hydrophila infection. Anim. Feed Sci. Technol. 2016, 211, 137– 144, DOI: 10.1016/j.anifeedsci.2015.11.004
16. Dien, L. T.; Ngo, T. P. H.; Nguyen, T. V.; Kayansamruaj, P.; Salin, K. R.; Mohan, C. V.; Rodkhum, C.; Dong, H. T. Non-antibiotic approaches to combat motile Aeromonas infections in aquaculture: Current state of knowledge and future perspectives. Rev. Aquacult. 2023, 15 (1), 333– 366, DOI: 10.1111/raq.12721
17. Lainioti, G. C.; Tsapikouni, A.; Druvari, D.; Avramidis, P.; Prevedouros, I.; Glaropoulos, A.; Kallitsis, J. K. Environmentally Friendly Cross-Linked Antifouling Coatings Based on Dual Antimicrobial Action. Int. J. Mol. Sci. 2021, 22 (9), 4658, DOI: 10.3390/ijms22094658
18. Namivandi-Zangeneh, R.; Wong, E. H. H.; Boyer, C. Synthetic Antimicrobial Polymers in Combination Therapy: Tackling Antibiotic Resistance. ACS Infect. Dis. 2021, 7 (2), 215– 253, DOI: 10.1021/acsinfecdis.0c00635
19. Li, W.; Hadjigol, S.; Mazo, A. R.; Holden, J.; Lenzo, J.; Shirbin, S. J.; Barlow, A.; Shabani, S.; Huang, T.; Reynolds, E. C.Star-Peptide Polymers are Multi-Drug-Resistant Gram-Positive Bacteria Killers. ACS Appl. Mater. Interfaces 2022, 14 (22), 25025– 25041, DOI: 10.1021/acsami.1c23734
20. Zhang, H.; Chen, Q.; Xie, J.; Cong, Z.; Cao, C.; Zhang, W.; Zhang, D.; Chen, S.; Gu, J.; Deng, S.Switching from membrane disrupting to membrane crossing, an effective strategy in designing antibacterial polypeptide. Sci. Adv. 2023, 9 (4), eabn0771 DOI: 10.1126/sciadv.abn0771
21. Zhou, M.; Qian, Y.; Xie, J.; Zhang, W.; Jiang, W.; Xiao, X.; Chen, S.; Dai, C.; Cong, Z.; Ji, Z.Poly(2-Oxazoline)-Based Functional Peptide Mimics: Eradicating MRSA Infections and Persisters while Alleviating Antimicrobial Resistance. Angew. Chem., Int. Ed. 2020, 59 (16), 6412– 6419, DOI: 10.1002/anie.202000505
22. Zhou, M.; Liu, L.; Cong, Z.; Jiang, W.; Xiao, X.; Xie, J.; Luo, Z.; Chen, S.; Wu, Y.; Xue, X.A dual-targeting antifungal is effective against multidrug-resistant human fungal pathogens. Nat. Microbiol. 2024, 9, 1325– 1339, DOI: 10.1038/s41564-024-01662-5
23. Bai, S.; Wang, J.; Yang, K.; Zhou, C.; Xu, Y.; Song, J.; Gu, Y.; Chen, Z.; Wang, M.; Shoen, C.A polymeric approach toward resistance-resistant antimicrobial agent with dual-selective mechanisms of action. Sci. Adv. 2021, 7 (5), eabc9917 DOI: 10.1126/sciadv.abc9917

24. Wiegand, I.; Hilpert, K.; Hancock, R. E. W. Agar and broth dilution methods to determine the minimal inhibitory concentration (MIC) of antimicrobial substances. Nat. Protoc. 2008, 3 (2), 163– 175, DOI: 10.1038/nprot.2007.521
25. Sudheesh, P. S.; Al-Ghabshi, A.; Al-Mazrooei, N. A. M.; Al-habsi, S. Comparative Pathogenomics of Bacteria Causing Infectious Diseases in Fish. Int. J. Evol. Biol. 2012, 2012, 457264, DOI: 10.1155/2012/457264
26. Chen, X.; Zhou, C.; Wang, J.; Wu, T.; Lei, E.; Wang, Y.; Huang, G.; Yu, Y.; Cai, Q.; Pu, H.Improving the Hemocompatibility of Antimicrobial Peptidomimetics through Amphiphilicity Masking Using a Secondary Amphiphilic Polymer. Adv. Healthcare Mater. 2022, 11 (15), e2200546 DOI: 10.1002/adhm.202200546
27. Chen, Z.; Zhang, W.; Chen, Y.; Wang, Y.; Bai, S.; Cai, Q.; Pu, H.; Wang, Z.; Feng, X.; Bai, Y. Alternatingly Amphiphilic Antimicrobial Oligoguanidines:Structure-Property Relationship and Usage as the Coating Materialwith Unprecedented Hemocompatibility. Chem. Mater. 2022, 34 (8), 3670– 3682, DOI: 10.1021/acs.chemmater.1c04331
28. Zhou, C.; Zhou, Y.; Zheng, Y.; Yu, Y.; Yang, K.; Chen, Z.; Chen, X.; Wen, K.; Chen, Y.; Bai, S.Amphiphilic Nano-Swords for Direct Penetration and Eradication of Pathogenic Bacterial Biofilms. ACS Appl. Mater. Interfaces 2023, 15 (16), 20458– 20473, DOI: 10.1021/acsami.3c03091
29. Wang, J.; Song, J.; Chen, X.; Guo, R.-T.; Wang, Y.; Huang, G.; Zheng, N.; Hu, P.; Feng, X.; Bai, Y. Multivalent Display of Lipophilic DNA Binders for Dual-Selective Anti-Mycobacterium Peptidomimetics with Binary Mechanism of Action. CCS Chem. 2022, 4 (11), 3573– 3586, DOI: 10.31635/ccschem.021.202101416
30. Epand, R. F.; Savage, P. B.; Epand, R. M. Bacterial lipid composition and the antimicrobial efficacy of cationic steroid compounds (Ceragenins). Biochim. Biophys. Acta, Biomembr. 2007, 1768 (10), 2500– 2509, DOI: 10.1016/j.bbamem.2007.05.023
31. Rathinam, V. A. K.; Zhao, Y.; Shao, F. Innate immunity to intracellular LPS. Nat. Immunol. 2019, 20 (5), 527– 533, DOI: 10.1038/s41590-019-0368-3
32. Little, J. W.; Edmiston, S. H.; Pacelli, L. Z.; Mount, D. W. Cleavage of the Escherichia coli lexA protein by the recA protease. Proc. Natl. Acad. Sci. U.S.A. 1980, 77 (6), 3225– 3229, DOI: 10.1073/pnas.77.6.3225
33. Kohanski, M. A.; Dwyer, D. J.; Hayete, B.; Lawrence, C. A.; Collins, J. J. A common mechanism of cellular death induced by bactericidal antibiotics. Cell 2007, 130 (5), 797– 810, DOI: 10.1016/j.cell.2007.06.049
34. Dwyer, D. J.; Belenky, P. A.; Yang, J. H.; MacDonald, I. C.; Martell, J. D.; Takahashi, N.; Chan, C. T. Y.; Lobritz, M. A.; Braff, D.; Schwarz, E. G.Antibiotics induce redox-related physiological alterations as part of their lethality. Proc. Natl. Acad. Sci. U.S.A. 2014, 111 (20), E2100– E2109, DOI: 10.1073/pnas.1401876111

35. Ma, P.; Wu, Y.; Jiang, W.; Shao, N.; Zhou, M.; Chen, Y.; Xie, J.; Qiao, Z.; Liu, R. Biodegradable peptide polymers as alternatives to antibiotics used in aquaculture. Biomater. Sci. 2022, 10 (15), 4193– 4207, DOI: 10.1039/D2BM00672C
36. Xiong, M.; Lee, M. W.; Mansbach, R. A.; Song, Z.; Bao, Y.; Peek, R. M.; Yao, C.; Chen, L.-F.; Ferguson, A. L.; Wong, G. C. L.Helical antimicrobial polypeptides with radial amphiphilicity. Proc. Natl. Acad. Sci. U.S.A. 2015, 112 (43), 13155– 13160, DOI: 10.1073/pnas.1507893112
37. Li, F.; Lin, L.; Chi, J.; Wang, H.; Du, M.; Feng, D.; Wang, L.; Luo, R.; Chen, H.; Quan, G.Guanidinium-rich lipopeptide functionalized bacteria-absorbing sponge as an effective trap-and-kill system for the elimination of focal bacterial infection. Acta Biomater. 2022, 148, 106– 118, DOI: 10.1016/j.actbio.2022.05.052
38. Maure, A.; Robino, E.; Van der Henst, C. The intracellular life of Acinetobacter baumannii. Trends Microbiol. 2023, 31 (12), 1238– 1250, DOI: 10.1016/j.tim.2023.06.007
39. Copp, J. N.; Pletzer, D.; Brown, A. S.; Van der Heijden, J.; Miton, C. M.; Edgar, R. J.; Rich, M. H.; Little, R. F.; Williams, E. M.; Hancock, R. E. W.Mechanistic Understanding Enables the Rational Design of Salicylanilide Combination Therapies for Gram-Negative Infections. Mbio 2020, 11 (5), e02068 DOI: 10.1128/mbio.02068-20

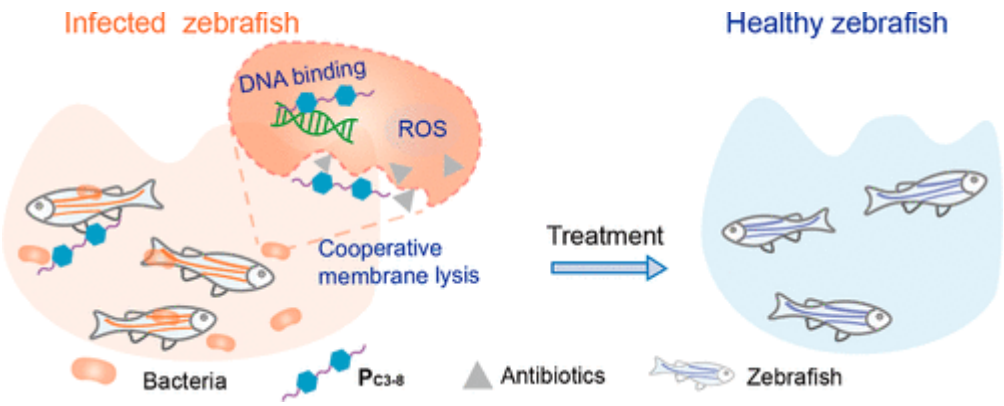

Figure 1. Schematic representation for the dual-targeting antimicrobial mechanism and synergistic effects of $\mathbf{P_{C3-8}}$ in combination with antibiotics against fish pathogens.

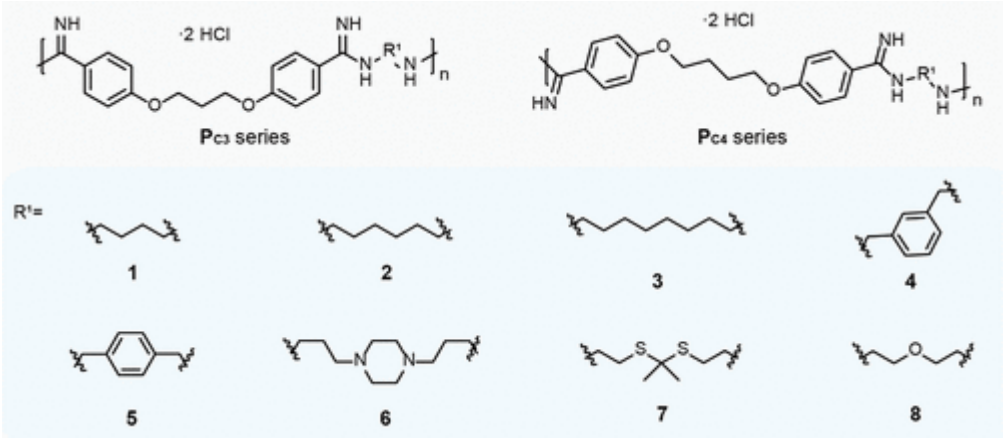

Figure 2. Molecular structures of $\mathbf{P_C}$-series polymers.

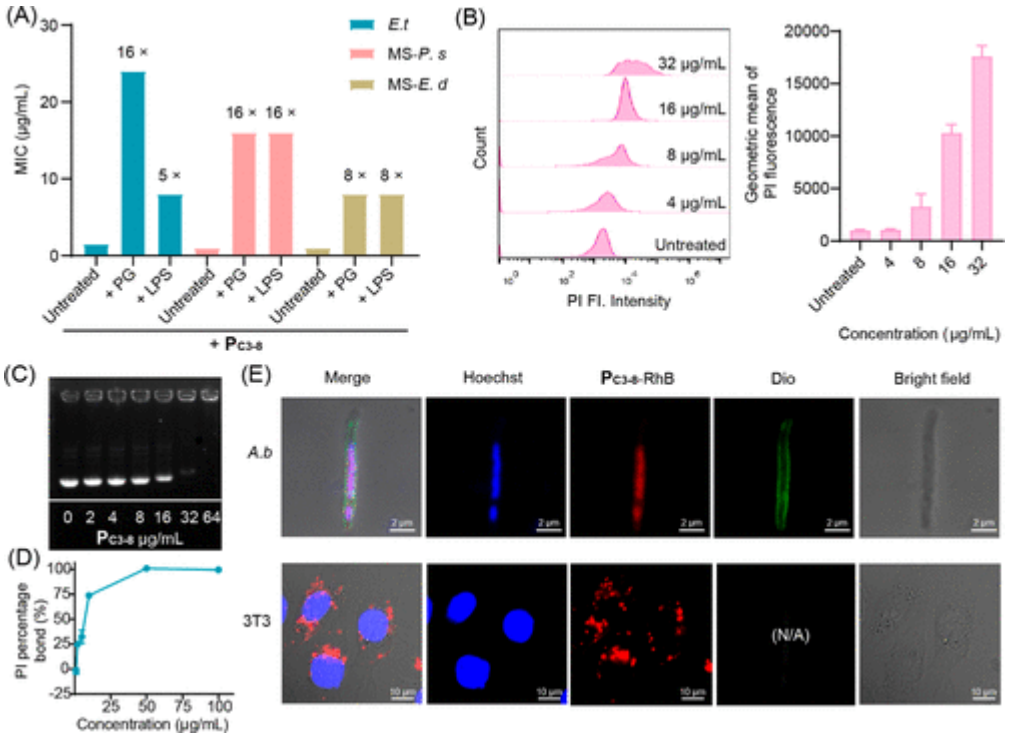

Figure 3. Evidence supports two distinct mechanisms of action for **$P_{C3–8}$**: membrane disruption and DNA binding. (A) Impact of exogenous PG and LPS on the MIC of **$P_{C3–8}$** against *E. t*, MS-*P. s*, or MS-*E. d*. (B) Membrane permeability assays of *E. c* cells with PI staining to illustrate the bacterial cell membrane disruption induced by the addition of **$P_{C3–8}$**. (C) Gel retardation assay employing **$P_{C3–8}$** and a plasmid DNA labeled with Gel-Red, demonstrating the ability of **$P_{C3–8}$** to retard DNA migration and displace Gel-Red. (D) Replacement of bound PI on pCold-ctx-m-15 plasmid DNA by **$P_{C3–8}$**, as evidenced in a fluorescence titration experiment. (E) Visualization of intracellular localization of **$P_{C3–8}$** in *A. b* cells and in NIH/3T3. Data shown in (B,D) are presented as the mean ± s.d. of at least 2 independent experiments.

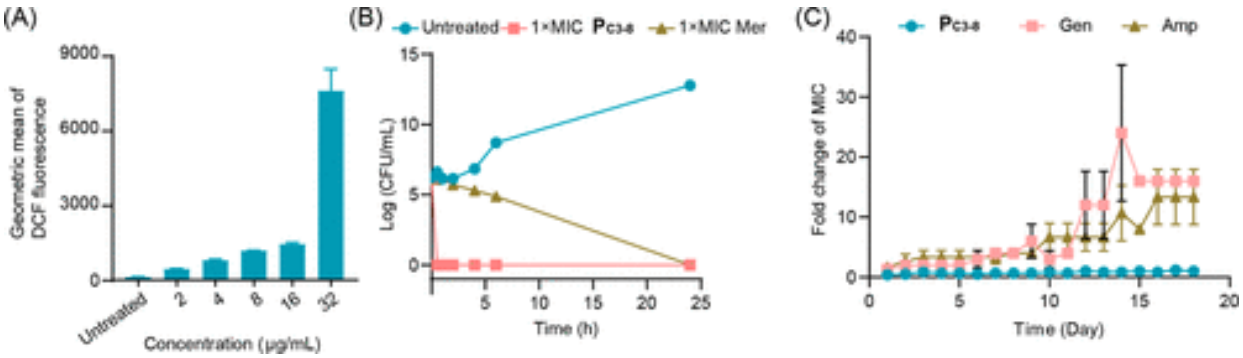

Figure 4. Antibacterial mechanism of **$P_{C3–8}$** in generating of ROS. (A) ROS generation by **$P_{C3–8}$** at 16 μg/mL in *E. c* probed by DCFH-DA. (B) Killing kinetics of **$P_{C3–8}$** (4 μg/mL) and Meropenem (Mer, 2 μg/mL) against *A. b*. (C) Resistance evolution profiles for **$P_{C3–8}$**, Gentamicin (Gen), and Ampicillin (Amp) against *E. c*. Data shown in (A–C) are presented as the mean ± s.d. of at least two independent experiments.

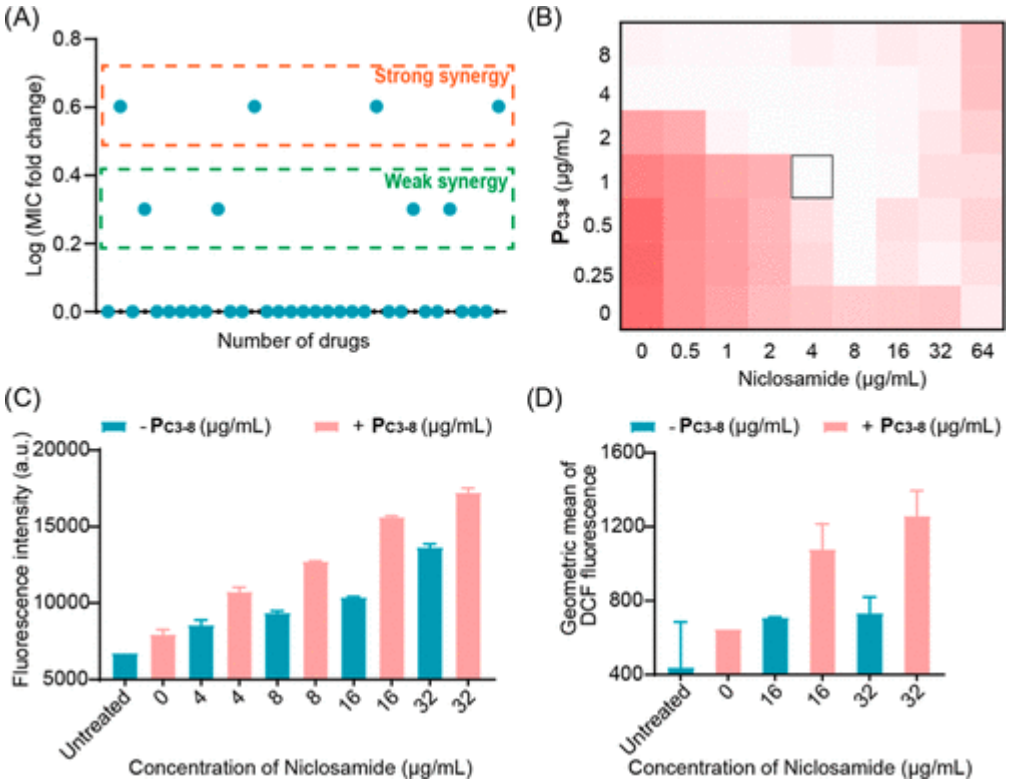

Figure 5. Study of synergistic effects with $\mathbf{P_{C3–8}}$ as a sensitizer. (A) Fold change in MICs of 33 normal antibiotics was combined with 1/4 MIC of $\mathbf{P_{C3–8}}$ against *E. t*. (B) Checkerboard assays of Niclosamide in combination with $\mathbf{P_{C3–8}}$ against *E. t*. (C) Membrane permeability assays of *E. t* cells with PI staining to illustrate the bacterial cell membrane disruption induced by the addition of $\mathbf{P_{C3–8}}$ (4 μg/mL), Niclosamide or their combination. (D) ROS generation by $\mathbf{P_{C3–8}}$, Niclosamide or their combination in *E. t* probed by DCFH-DA. Note: at high concentrations, Niclosamide exhibited poor solubility in the CAMHB medium, leading to precipitation and higher OD readings in Figure 5B.

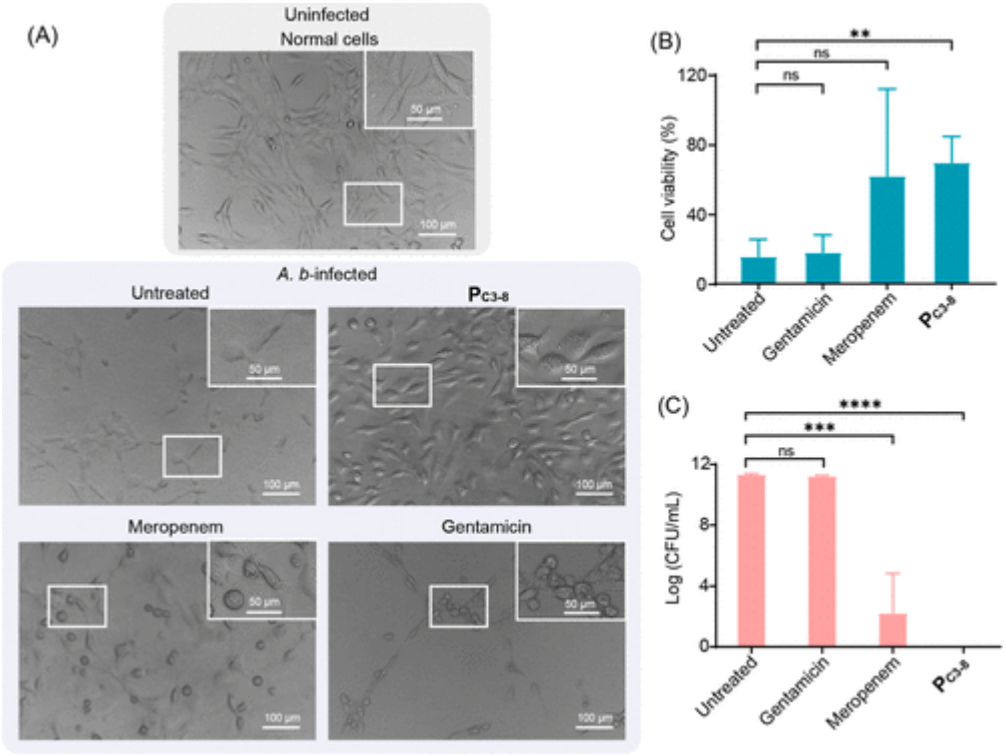

Figure 6. Antibacterial effects of **$P_{C3–8}$** in ex vivo infection models. (A) Images of the rescue effect with **$P_{C3–8}$** (8 μg/mL), Meropenem (8 μg/mL), and Gentamicin (8 μg/mL) on MDR *A. b*-infected NIH/3T3 cells. (B) Cell viability of NIH/3T3 cells treated with **$P_{C3–8}$** or antibiotics. (C) Quantitative analysis of the cell rescue effect in the bacterium-cell coculture model study, comparing **$P_{C3–8}$** and antibiotics. Data shown in (B,C) are presented as the mean ± standard deviation of at least 2 independent experiments. Statistical significances were analyzed using student's *t*-test, and significant differences between groups are marked with an asterisk. ns, **, ***, and **** indicate $P > 0.05$, $P \leq 0.01$, $P \leq 0.001$, and $P \leq 0.0001$, respectively.

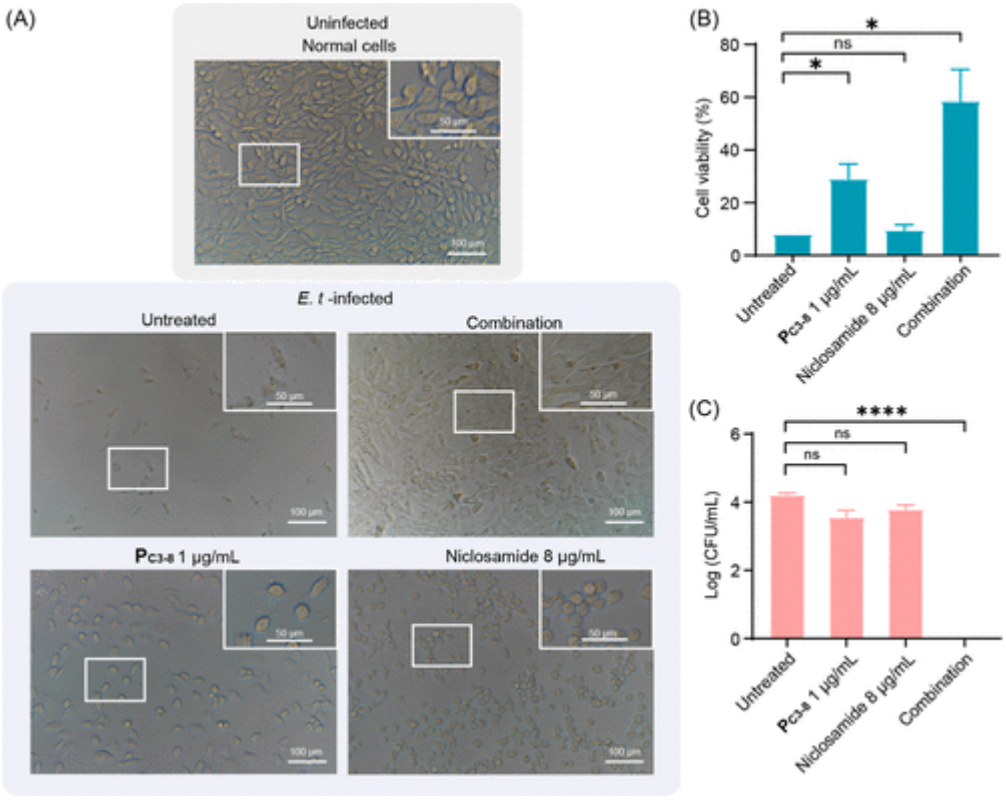

Figure 7. Antibacterial effects of **$P_{C3–8}$** in ex vivo infection models. (A) Images of rescue effect of **$P_{C3–8}$** on *E. t*-infected NIH/3T3 cells. (B) Quantitative analysis of the cell rescue effect in the bacterium-cell coculture model study, comparing **$P_{C3–8}$**, Niclosamide or their combination. (C) Cell viability of NIH/3T3 cells treated with **$P_{C3–8}$**, Niclosamide, or their combination. Data shown in (B,C) are presented as the mean ± s.d. of at least 2 independent experiments. Statistical significances were analyzed using the student's *t*-test and significant differences between groups are marked with an asterisk. ns, **, *** and **** indicate $P > 0.05$, $P \leq 0.01$, $P \leq 0.001$, and $P \leq 0.0001$, respectively.

Figure 8. Antibacterial effects of **$P_{C3–8}$** *in vivo* infection models. (A) Illustrative depiction of medication rescue for zebrafish following bacterial infection is presented. (B) Survival of *E. t*-infected zebrafish after various treatments (2 μg/mL). (Statistical significances were analyzed using student's *t*-test, and significant differences between groups are marked with an asterisk. ns, **, ***, and **** indicate $P > 0.05$, $P \leq 0.01$, $P \leq 0.001$, and $P \leq 0.0001$, respectively.).

Table 1. MIC of $P_{C3–8}$ against *E. tarda* (*E. t*)

polymers	MIC (μg/mL)	polymers	MIC (μg/mL)
$P_{C3–1}$	6	$P_{C4–1}$	8
$P_{C3–2}$	8	$P_{C4–2}$	8
$P_{C3–3}$	8	$P_{C4–3}$	8
$P_{C3–4}$	16	$P_{C4–4}$	24
$P_{C3–5}$	16	$P_{C4–5}$	16
$P_{C3–6}$	4	$P_{C4–6}$	16
$P_{C3–7}$	16	$P_{C4–7}$	8
$P_{C3–8}$	4	$P_{C4–8}$	8

$P_{C3–8}$ was then tested against various bacterial strains. The results are given in Table 2. **$P_{C3–8}$** was found to exhibit potent antibacterial activity against both Gram-negative and Gram-positive bacteria. **$P_{C3–8}$** against *E. c*, *A. b*, and *K. pneumoniae* (*K. p*) showed MIC values ranged from 1 to 4 μg/mL. It exhibited superior effects, particularly on clinical strain isolates with multidrug resistance (Table S3). For Gram-positive bacteria, including the multidrug-resistant *S. a* (*S. a*-MDR), the MIC values were found in the range of 0.5–2 μg/mL. Notably, **$P_{C3–8}$** also demonstrated promising antibacterial activity against *Mycobacterium* species, with MIC values ranging from 0.25 to 2 μg/mL, despite some strains like *M. smegmatis* being nonpathogenic.

Table 2. MIC of P_{C3-8} against Different Bacterial Strains, including Gram-Positive, Gram-Negative, *Mycobacterium*, and Isolates from *M. salmoides*[c]

bacteria		MIC (μg/mL)
Gram positive	*E. f*	2
	B. s	0.5
	S. a	1
	S. a-MDR[a]	1
	MRSA	2
Gram negative	MS[b]-*A. h*	1
	MS-*P. s*	1
	MS-*V. h*	3
	MS-*E. d*	1
	E. t	4
	E. c	2
	E. c-MDR	1
	K. p	1
	K. p-MDR	4
	A. b	4
	A. b-MDR	4
	P. a	4
	P. a-MDR	16
Mycobacterium	*M. f*	2
	M. s	0.25

[a] Strains having their names ending with-MDR are clinical is olates with multidrug resistance.

[b] Strains having their names starting with MS-belong to the species *M. salmoides*.

[c] *E. faecalis* (*E. f*); *B. subtilis* (*B. s*); *S. aureus* (*S. a*); Methicillin-resistant *S. aureus* strain (MRSA); *M. salmoides-A. hydrophila* (MS-*A. h*); *M. salmoides-P. Shigelloides* (MS-*P. s*); *M. salmoides-A. veronii* (MS-*V. h*); *M. salmoides-E. dwardsiella* (MS-*E. d*); *E. tarda* (*E. t*); *E. coli* (*E. c*); *K. pneumoniae* (*K. p*); *A. baumannii* (*A. b*); *P. aeruginosa* (*P. a*); *Mycobacterium fortuitum* (*M. f*); and *M. smegmatis* (*M. s*). Both laboratory strains and multidrug-resistant clinical isolates were evaluated to fully assess the antibacterial spectrum.